Singularity spectrum of a critical KAM torus

1987 J. Phys. A: Math. Gen. 20 L953

(http://iopscience.iop.org/0305-4470/20/15/004)

J. Phys. A: Math. Gen. **20** (1987) L953-958. Printed in the UK

LETTER TO THE EDITOR

Singularity spectrum of a critical KAM torus

A H Osbaldestin and M Y Sarkis

Mathematics Department, Loughborough University of Technology, Loughborough, Leicestershire LE11 3TU, UK

Received 30 March 1987, in final form 26 June 1987

Abstract. We numerically determine the $f(\alpha)$ spectrum of scaling indices for critical KAM tori in the area-preserving standard map. Similarities and differences between the corresponding orbits of circle maps are discussed.

Recently, Halsey *et al* [1] have introduced a method of describing the global behaviour of certain strange orbits arising in dynamical systems (see also [2]). One of the examples studied in [1] is the golden mean orbit for circle maps at the onset of chaos. It is found that the variations in density of the orbit points on the circle are describable by a universal smooth spectrum of scaling indices known as the $f(\alpha)$ spectrum. The density of points within a small distance l around a point x_i is denoted $p_i(l)$ and the corresponding index α_i is defined by $p_i(l)=l^{\alpha_i(l)}$. It is found that α_i lies in an interval $[\alpha_{\min}, \alpha_{\max}]$ whose endpoints are determined by the scaling behaviour at the critical point of the map. $f(\alpha)$ is the Hausdorff dimension of the set of points on the circle having index α.

The formalism has also been applied to the attractor at the accumulation of period doubling bifurcations [1], the mode-locking structure of circle maps at the onset of chaos [1], the spectrum of a quasiperiodic Schrödinger operator [3] and the critical point orbit on the boundary of a Siegel disc [4].

It is the purpose of this letter to report on the application of this analysis to the critical golden mean KAM torus in the area-preserving standard map.

The standard map:

$$\begin{aligned} r_{n+1} &= r_n-(k/2\pi)\sin(2\pi\theta_n) \\ \theta_{n+1} &= \theta_n+r_{n+1} \qquad \bmod 1 \end{aligned} \tag{1}$$

has been a valuable model for the behaviour of Hamiltonian systems (see for instance [5]). Of particular interest is the transition to 'global stochasticity', i.e. the breakup of the last rotational invariant circle. It appears that there is a circle up to $k=k_c\simeq 0.971\,635\,406$ of rotation number $\gamma=\frac{1}{2}(\sqrt{5}-1)$, the reciprocal of the golden mean [6]. For brevity we call this the golden circle.

In many ways this situation is similar to the persistence of dense orbits of rotation number γ up to the critical perturbation $k=1$ in the 'sine circle map':

$$\theta_{n+1}=\theta_n+\Omega-(k/2\pi)\sin(2\pi\theta_n) \tag{2}$$

as studied in [1]. There are important differences, however.

(D1) The presence of symmetry lines in the standard map [7]. Figure 1(a) shows the distribution of points of the critical golden orbit. There is symmetry about $\theta=0$

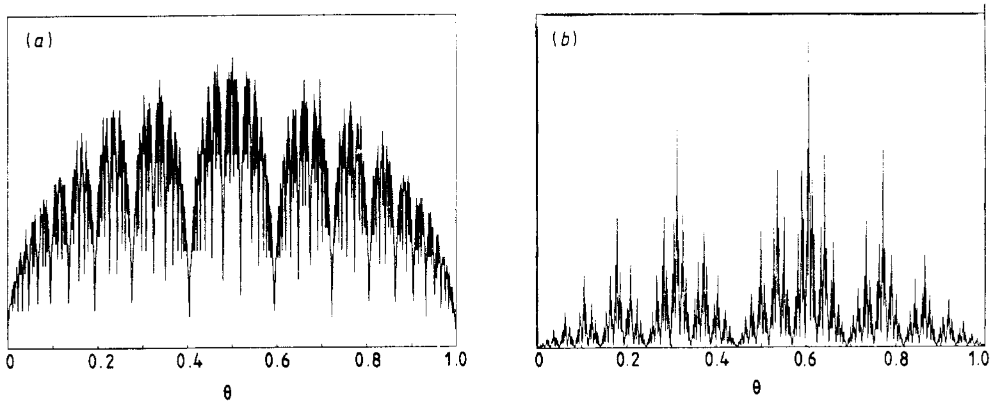

Figure 1. (a) The histogram obtained from several thousand iterates of the point of the critical golden circle on the line $\theta = 0$ in the standard map (1). (b) The histogram from several thousand iterates of the critical point of the circle map (2).

and $\theta = 0.5$. Figure 1(b) shows the distribution for the analogous orbit of the circle map (2).

(D2) The induced circle map on the critical KAM torus is believed to be only once continuously differentiable for the standard map golden circle [8]. Moreover, it has no critical points. The critical circle map, $k = 1$ in (2), has a cubic inflection at $\theta = 0$. Figure 2(a) shows the induced return map on the critical golden circle and figure 2(b) its derivative.

The algorithm described in [1] to calculate the $f(\alpha)$ spectrum consists of the following steps. We take a critical orbit (r_0, θ_0), $(r_1, \theta_1), \ldots, (r_i, \theta_i), \ldots$ truncated at $i = F_n$ (F_n is a Fibonacci number) and form the lengths $l_i = \mathrm{d}((r_i, \theta_i), (r_{i+F_{n-1}}, \theta_{i+F_{n-1}}))$ (with $\theta_{i+F_{n-1}} - \theta_i$ calculated mod 1). These lengths serve as natural scales for a partition with measures $p_i = 1/F_n$ associated with each scale.

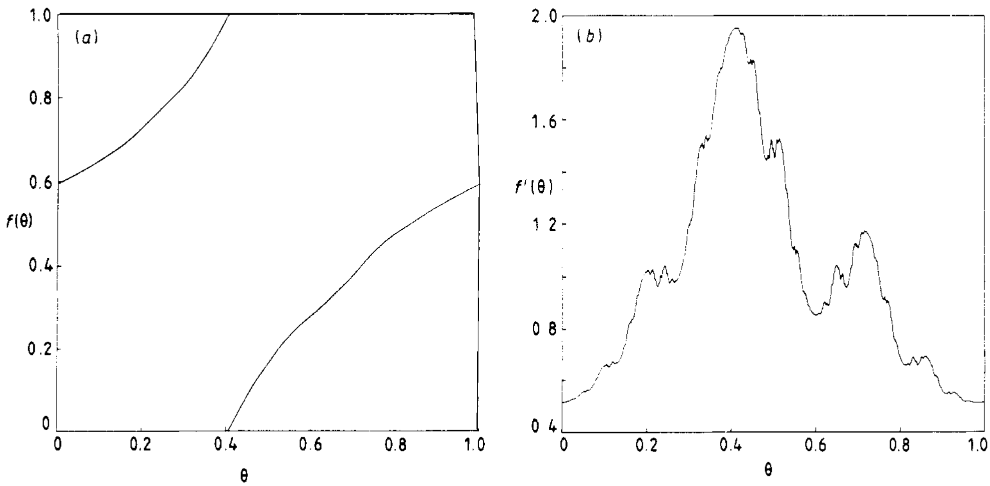

Figure 2. (a) The critical golden circle of the standard map in the θ_n, θ_{n+1} plane, i.e. the graph of the induced return map. (b) The derivative of the curve in (a). Note there are no zeros and that the curve appears continuous but not differentiable.

From these lengths we form the partition function

$$\Gamma_n(q, \tau) = \sum_{i=1}^{F_n} \frac{p_i^q}{l_i^\tau} \tag{3}$$

and Halsey *et al* [1] argue that, for large n, this is of order unity only when

$$\tau = (q-1)D(q) \tag{4}$$

with $D(q)$ related to a set of dimensions introduced by Renyi [9] (see also Hentschel and Procaccia [10]). For instance, with $q=0$, $\tau=-D(0)$ and $\Gamma_n=1$ is an implicit equation for $D(0)$ the Hausdorff dimension. $D(1)$ is the information dimension and $D(2)$ the correlation exponent [10].

The dimensions $D(q)$ are decreasing with q, and f and α are given via the Legendre transformation

$$\alpha(q) = \mathrm{d}\tau/\mathrm{d}q \tag{5}$$

$$f(q) = \tau - q\,\mathrm{d}\tau/\mathrm{d}q. \tag{6}$$

Eliminating q gives the function $f(\alpha)$ defined on a range $[\alpha_{\min}, \alpha_{\max}]$.

In practice, the solutions to $\Gamma_n = 1$ converge slowly with n and it is better to solve the equation

$$\Gamma_n/\Gamma_{n-1} = 1 \tag{7}$$

somewhat reminiscent of the finite-size scaling method in statistical mechanics (see for instance [11]).

We see from the histogram of figure 1(a) that the minimum density is at $\theta=0$ and the maximum density occurs at $\theta=0.5$. Unlike the circle map, since $\theta=0$ is not a critical point of the return map, its iterate ($\theta=r_0\simeq 0.594\,920\,91$) is not a density maximum but is also a minimum. The local scaling behaviour at the minimum and maximum density points determines the range of $D(q)$ as q varies from $-\infty$ to $+\infty$ and hence determines the range $[\alpha_{\min}, \alpha_{\max}]$.

The local scaling behaviour around $\theta=0$ and $\theta=0.5$ has been determined by Shenker and Kadanoff [7], who find a universal value for the limiting ratio of successive Fibonacci iterate distances from the starting point.

Starting on the axis $\theta=0$, for the golden mean, γ, it is found that

$$\lim_{n\to\infty} \frac{d_n(0)}{d_{n+1}(0)} = \gamma^{-x_0} \tag{8}$$

where $d_n(\theta_0)$ is the distance of the F_nth iterate of the starting point on the line $\theta=\theta_0$ from that starting point and $x_0\simeq 0.721$.

Around $\theta=0.5$ this equation must be modified slightly; convergence is witnessed only if we step by three, due to the routing pattern of the orbit [7]. It is found that

$$\lim_{n\to\infty} \frac{d_n(0.5)}{d_{n+3}(0.5)} = \gamma^{-x_1} \tag{9}$$

with $x_1\simeq 1.093$.

The exponents x_0 and x_1 are precisely what we need to determine $\alpha_{\min}$ and $\alpha_{\max}$. Indeed, following Halsey *et al* [1], we have

$$D(-\infty) = \alpha_{\max} = \frac{\ln\gamma}{\ln(\gamma^{x_0})} = \frac{1}{x_0} \simeq 1.387 \tag{10}$$

and

$$D(\infty) = \alpha_{\min} = \frac{\ln \gamma}{\ln(\gamma^{x_1})} = \frac{1}{x_1} \simeq 0.915. \tag{11}$$

The stepping by three in equation (9) indicates that we ought to modify equation (7) to obtain sensible numerical results for large positive q. We therefore numerically solve the equation

$$\Gamma_n/\Gamma_{n-3} = 1 \tag{12}$$

for $D(q)$ as a function of q via equation (4). Figure 3 is a plot of the function $D(q)$ thus obtained. Its Legendre transform (equations (5) and (6)) gives the $f(\alpha)$ graph and is shown in figure 4. Excellent agreement with the predicted values of $\alpha_{\min}$ and $\alpha_{\max}$ ((10) and (11)) is seen. Note that the maximum value of f, which occurs when $q=0$ (here $\alpha \simeq 1.01$), is the fractal dimension of the torus which is one here. Despite the fact that the critical orbit is 'strange', the dynamics still takes place on a set with integer dimension.

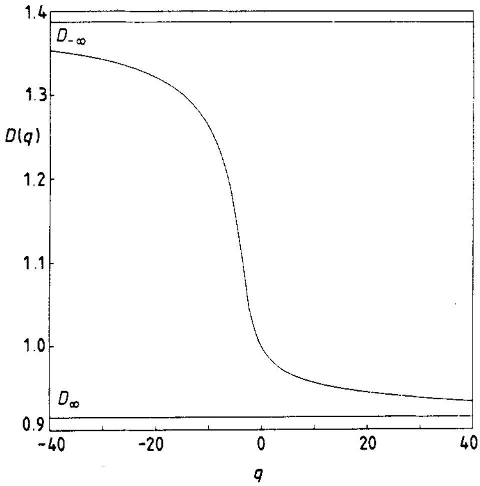

Figure 3. The graph of $D(q)$ for the critical golden circle.

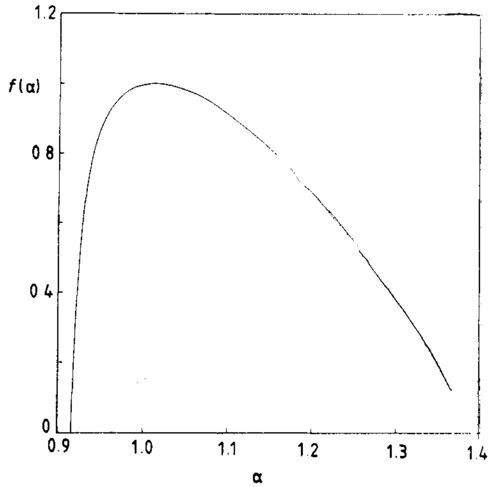

Figure 4. The graph of $f(\alpha)$ for the critical golden circle.

We have also investigated two other rotation numbers with different routing patterns: (a) $\sqrt{2}-1$ with continued fraction expansion $[2, 2, 2, \ldots]$ and (b) $\sqrt{3}-1$ with expansion $[1, 2, 1, 2, \ldots]$. In both of these examples the maximum density is not at $\theta = 0.5$ (figure 5) but appears to be on one of the other symmetry lines of the standard map (the lines $\theta = \frac{1}{2}r$ or $\theta = \frac{1}{2}(r+1)$). The exponent x_1 of Shenker and Kadanoff [7] is not expected to give $\alpha_{\min}$, but instead it is necessary to calculate the local scaling behaviour at the point where the torus crosses the appropriate symmetry line. Equations (8) and (9) must be modified when the continued fraction expansion has period greater than one with the rotation number replaced by $\lim_{n\to\infty}(q_n/q_{n+s})$, with (q_n) the denominators of the convergents of the rotation number and s the period of the continued fraction expansion ($=2$ for $\sqrt{3}-1$) [8].

Figure 6 shows the $f(\alpha)$ curve for these two rotation numbers. The scaling exponent x_0 is common to all rotation numbers considered here and hence so is $\alpha_{\max}$. However

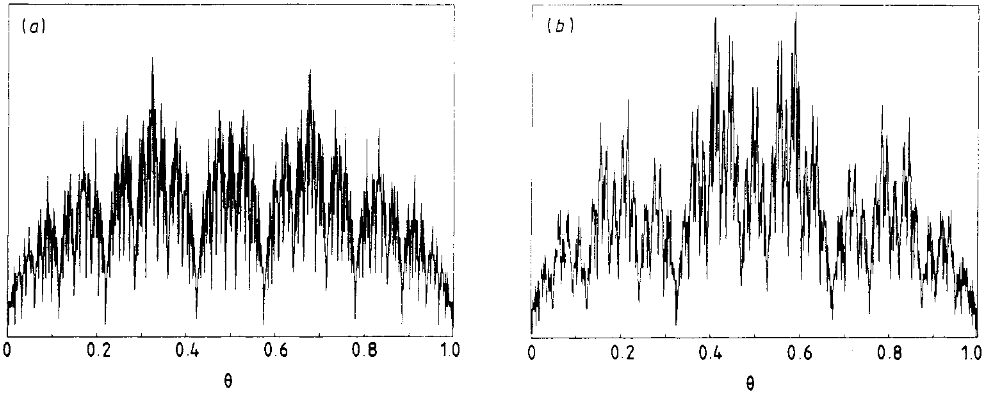

Figure 5. The histogram of several thousand iterates on the critical torus of (*a*) rotation number $\sqrt{2}-1$, (*b*) rotation number $\sqrt{3}-1$.

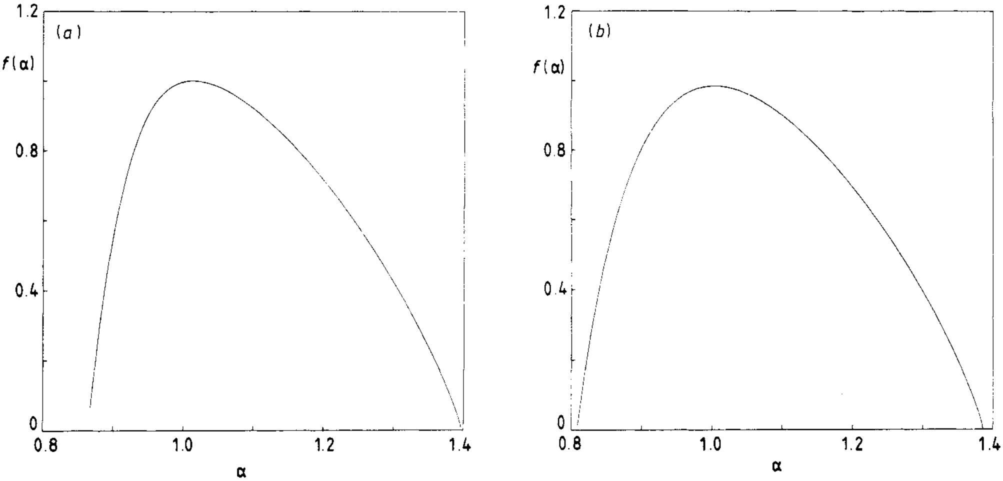

Figure 6. The $f(\alpha)$ graph for (*a*) the critical $\sqrt{2}-1$ torus and (*b*) the critical $\sqrt{3}-1$ torus.

$\alpha_{\min}$ differs in all three cases. This is distinct from the critical circle map ($k=1$ in (2)) where $\alpha_{\min}=\frac{1}{3}\alpha_{\max}$ always (three being the degree of the inflection).

References

[1] Halsey T C, Jensen M H, Kadanoff L P, Procaccia I and Shraiman B I 1986 *Phys. Rev.* A **33** 1141

[2] Frisch U and Parisi G 1985 *Turbulence and Predictability in Geophysical Fluid Dynamics and Climate Dynamics. Proc. Enrico Fermi Int. School of Physics, Course LXXXVIII* ed M Ghil (Amsterdam: North-Holland) p 84

[3] Tang C and Kohmoto M 1986 *Phys. Rev.* B **34** 2041

[4] Osbaldestin A H 1987 unpublished

[5] Lichtenberg A J and Liebermann M A 1983 *Regular and Stochastic Motion* (*Appl. Math. Sci.* **38**) (Berlin: Springer)

[6] Greene J M 1979 *J. Math. Phys.* **20** 1183

[7] Shenker S J and Kadanoff L P 1982 *J. Stat. Phys.* **27** 631
[8] Ostlund S, Rand D, Sethna J and Siggia E 1983 *Physica* **8D** 303
[9] Renyi A 1976 *Selected Papers* vol 2 (Budapest: Akademiai Kiodo) p 526
[10] Hentschel H G E and Procaccia I 1983 *Physica* **8D** 435
[11] Barber M N 1983 *Phase Transitions and Critical Phenomena* vol 8, ed C Domb and J L Lebowitz (New York: Academic) p 146